doi:10.1246/cl.2012.26

Published on the web December 24, 2011

A Dimer-of-dimers Composed of Paddlewheel Diruthenium(II, III) Complexes and a Bridge of Tetrachlorohydroquinonate(2−) Derived by Intramolecular Charge Transfers

Masahisa Itoh,[1] Yuichiro Asai,[1] Hiromichi Kamo,[1] Akira Miura,[1] and Hitoshi Miyasaka*[2]
[1]*Department of Chemistry, Graduate School of Science, Tohoku University,*
6-3 Aramaki-Aza-Aoba, Aoba-ku, Sendai, Miyagi 980-8578
[2]*Department of Chemistry, Division of Material Sciences, Graduate School of Natural Science and Technology,*
Kanazawa University, Kakuma, Kanazawa, Ishikawa 920-1192

(Received September 27, 2011; CL-110787; E-mail: miyasaka@se.kanazawa-u.ac.jp)

The reaction of a paddlewheel-type diruthenium(II, II) complex, $[Ru_2^{II,II}(o\text{-}MeOPhCO_2)_4(THF)_2]$ ($[Ru_2^{II,II}]$; $o\text{-}MeOPhCO_2^-$: *o*-anisate), and chloranil (QCl_4) leads to a charge transfer from $[Ru_2^{II,II}]$ to QCl_4, forming a dimer-of-dimers of $[Ru_2^{II,III}]^+$ units bridged by tetrachlorohydroquinonate dianion (QCl_4^{2-}): $[\{Ru_2^{II,III}(o\text{-}MeOPhCO_2)_4(THF)\}_2(QCl_4)]$.

A family of carboxylate-bridged paddlewheel diruthenium complexes (abbreviated henceforth as $[Ru_2]$) is not only a useful building block for constructing metal–organic frameworks but also a good functional module for functionalizing materials with electronic or magnetic characteristics.[1–7] A noteworthy functional property of $[Ru_2]$ is its redox activity reversibly changeable between $[Ru_2^{II,II}]$ and $[Ru_2^{II,III}]^+$, which concomitantly enables the variation of spin ground state between $S = 1$ and $S = 3/2$, respectively, without significant structural change. Recently, our group has demonstrated the utility of carboxylate-bridged $[Ru_2^{II,II}]$ complexes as a good electron-donor (D) module in charge-transfer systems with polycyano organic acceptors (A) such as 7,7,8,8-tetracyanoquinodimethane (TCNQ) and *N*,*N*′-dicyanoquinodiimine (DCNQI) derivatives, in which the D → A charge-transfer can be controlled by the combination of the ionization potential of D and the electron affinity of A.[8–10] Even in such covalently bonded D–A systems, magnetic and electron-transport properties of materials are closely associated with the intralattice D → A charge transfer. For a purpose of expanding D–A combinations, we have now chosen chloranil (QCl_4) as A, which can undergo two-step redox reaction to produce $QCl_4^{\bullet-}$ (Cl_4-semiquinonate) and QCl_4^{2-} (Cl_4-hydroquinonate) and have done an assembly reaction with a relatively strong donor, $[Ru_2^{II,II}(o\text{-}MeOPhCO_2)_4(THF)_2]$ ($o\text{-}MeOPhCO_2^-$: *o*-anisate, Figure S1[33]):[11] This reaction provided a discrete D:A = 2:1 assembly, $[\{Ru_2^{II,III}(o\text{-}MeOPhCO_2)_4\text{-}(THF)\}_2(QCl_4)]$ (**1**), involving a complete charge transfer to form QCl_4^{2-}.

Note that even though the reaction with a 1:1 molar mixture of the components is carried out in a benzene solution, independent of temperature, the final product **1** is always composed of a 2:1 ratio of $[Ru_2]$ and QCl_4, being a thermodynamically stable material (to increase the yield, it was finally carried out in a 2:1 molar ratio of $[Ru_2]/QCl_4$).[12] Crystals that are suitable for single-crystal X-ray crystallography were finally obtained by a slow diffusion of the components in benzene at an ambient temperature:[12] This material is isostructural with the material obtained from a hot benzene solution, as confirmed in X-ray powder reflection patterns (Figure S2[33]).

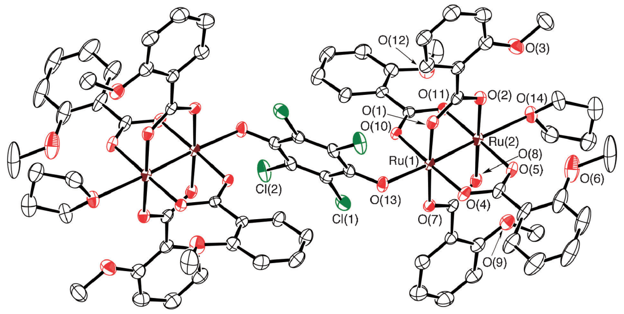

Figure 1. ORTEP plot of **1** (30% probability ellipsoids). Hydrogen atoms are omitted for clarity.

Compound **1** crystallizes in the monoclinic space group $P2_1/n$ with $Z = 2$.[13] The asymmetric unit is composed of a half of the formula unit, in which an inversion center is located at the midpoint of the QCl_4 moiety; that is, two $[Ru_2]$ units are crystallographically equivalent. Compound **1** has a dimer-of-dimers structural motif with a QCl_4 bridge, where one site of $[Ru_2]$ moieties is capped by THF (Figure 1). This type of discrete material is quite rare in cases using carboxylate-bridged $[Ru_2]$ complexes,[2,14] because high-symmetric $[Ru_2]$ units, in general, act as an edge of arrays as seen in most assembled materials,[8,10] and little is known about producing asymmetric axial coordinating sites in such $[Ru_2]$ units. This is very likely because the asymmetric geometry 4,0-$[Ru_2]$, which is defined by the orientation of MeO groups of *o*-anisate ligands, is consequently stabilized in the dimer-of-dimers form to avoid steric hindrance between $[Ru_2]$ units via a bridge of relatively small molecule of QCl_4. Indeed, the precursor, $[Ru_2^{II,II}(o\text{-}MeOPhCO_2)_4(THF)_2]$, takes a *cis*-2,2-$[Ru_2]$ configuration, which provides equivalent axial sites each coordinating THF (Figure S1[33]). For the bridging array of [THF–{Ru(2)–Ru(1)}–QCl_4–{Ru–Ru}–THF], relevant bond distances and angles are: Ru(1)–Ru(2) = 2.2774(5) Å, $\text{Ru(1)–O(13)}_{QCl_4}$ = 2.119(3) Å, Ru(2)–O(14)_{THF} = 2.344(3) Å, $\text{Ru(2)–Ru(1)–O(13)}_{QCl_4}$ = 176.47(8)°, $\text{Ru(1)–Ru(2)–O(14)}_{THF}$ = 174.32(7)°, $\text{Ru(1)–O(13)–C(33)}_{QCl_4}$ = 125.9(3)°. The bond lengths in the $[Ru_2]$ and QCl_4 moieties can be used to estimate the degree of charge transfer from $[Ru_2]$ to QCl_4. The Ru–O_{eq} (O_{eq}: carboxylate oxygen) bond length characteristically reflects the oxidation state of $[Ru_2]$, which is, in general, found in the range of 2.07–2.09 Å for $[Ru_2^{II,II}]$ and 2.01–2.03 Å for $[Ru_2^{II,III}]^+$.[15,16] The average Ru–O_{eq} length for $[Ru_2]$ in **1** is: 2.022 Å, which means the $[Ru_2^{II,III}]^+$ state (Table S1[33]). Note that the notation of mixed valency (e.g., II,III) is merely a formality for easily under-

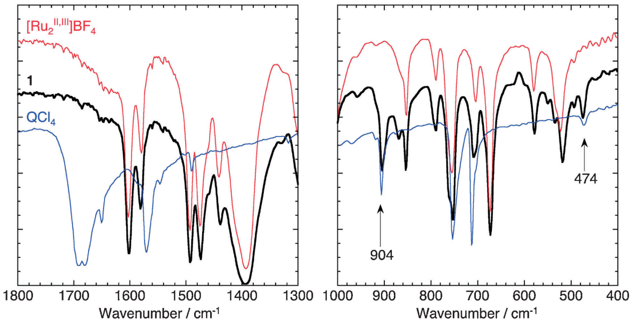

Figure 2. IR spectra of **1** (black) together with those of $\mathrm{QCl_4}$ (blue) and $[\mathrm{Ru_2^{II,III}}(o\text{-}\mathrm{MeOPhCO_2})_4(\mathrm{THF})_2]\mathrm{BF_4}$ (red).

standing the valence of $[\mathrm{Ru_2}]$ moiety: The nature of mixed-valency cannot be discussed in such metal–metal bonded families even if an asymmetric unit was formed. Considering the charge balance of the neutral material of **1**, the $\mathrm{QCl_4}$ moiety should be divalent (i.e., $\mathrm{QCl_4^{2-}}$). Table S1[33] shows bond distances of the $\mathrm{QCl_4}$ moiety in **1** ($\mathrm{C{-}O} = 1.314(5)$ Å, $\mathrm{C_O{-}C_{Cl}} = 1.418(5)$ and $1.407(4)$ Å, $\mathrm{C_{Cl}{-}C_{Cl}} = 1.380(6)$ Å) and relevant materials.[17–27] The C–O (*a*; see the figure in Table S1[33]) and C–C ($\mathrm{C_O{-}C_{Cl}}$, *b*; $\mathrm{C_{Cl}{-}C_{Cl}}$, *c*) bonds of $\mathrm{QCl_4}$ are characteristically changeable in a modification between quinonoid and benzenoid forms, in particular the C–C bonds accurately reflect the charge on an aromatic ring: The C–O distance in the benzenoid form of $\mathrm{QCl_4^{2-}}$ (ca. 1.27–1.33; single-bond character) is longer than that in the quinonoid form of $\mathrm{QCl_4^{0}}$ (ca. 1.20–1.23; double-bond character), and the C–C bonds of *b* and *c* (see the figure in Table S1[33]) tend to become equally in the benzenoid form of $\mathrm{QCl_4^{2-}}$ with $\Delta(b\text{–}c) \leq 0.1$, while they are clearly distinguishable in the semiquinonate form of $\mathrm{QCl_4^{\bullet-}}$ with $\Delta(b\text{–}c) \approx 0.1$ and quinonoid form of $\mathrm{QCl_4^{0}}$ with $(\Delta(b\text{–}c) > 0.13$ (Table S1[33]). These trends provide us a conclusion on $\mathrm{QCl_4}$ in **1** taking the benzenoid form with a valence of -2, i.e., hydroquinonate form ($\mathrm{QCl_4^{2-}}$).

To ascertain the charge distribution between $[\mathrm{Ru_2}]$ and $\mathrm{QCl_4}$ moieties, infrared spectra of **1** was measured on a KBr pellet, and Figure 2 shows those together with $\mathrm{QCl_4^{0}}$ and $[\mathrm{Ru_2^{II,III}}(o\text{-}\mathrm{MeOPhCO_2})_4(\mathrm{THF})_2]\mathrm{BF_4}$ newly synthesized for comparison (Figure S3[33]).[28] In general, *p*-quinones have a characteristic C–O stretching band at around $1630\text{–}1700\,\mathrm{cm^{-1}}$;[29] actually, $\mathrm{QCl_4^{0}}$ exhibits a strong band at ca. $1690\,\mathrm{cm^{-1}}$, which tends to shift ca. $150\,\mathrm{cm^{-1}}$ to a lower frequency in $\mathrm{QCl_4^{\bullet-}}$ and further to a lower frequency in $\mathrm{QCl_4^{2-}}$. No C=O stretching band was observed for **1**, but unfortunately, we also could not assign the C–O stretching band, because it seems as if there is no characteristic band for the C–O stretching in the typical range ($1420\text{–}1490\,\mathrm{cm^{-1}}$)[29] expected (left of Figure 2), although two bands at 474 and $904\,\mathrm{cm^{-1}}$ in **1** certainly originate from the $\mathrm{QCl_4^{2-}}$ moiety (right of Figure 2). A wide band observed at around $1350\text{–}1440\,\mathrm{cm^{-1}}$ may be overlapping it.

Figure 3 shows powder reflection spectra of **1**, together with those of $\mathrm{QCl_4}$, $[\mathrm{Ru_2^{II,II}}(o\text{-}\mathrm{MeOPhCO_2})_4(\mathrm{THF})_2]$, and $[\mathrm{Ru_2^{II,III}}(o\text{-}\mathrm{MeOPhCO_2})_4(\mathrm{THF})_2]\mathrm{BF_4}$ for comparison. Comparing those spectra, we can find a unique absorption for **1** at around $10900\,\mathrm{cm^{-1}}$ (1.35 eV), assignable to a $\mathrm{QCl_4^{2-}}$–to–$[\mathrm{Ru_2^{II,III}}]^+$ transition, proving the charge distribution of $[\{\mathrm{Ru_2^{II,III}}\}^+\text{–}(\mathrm{QCl_4^{2-}})\text{–}\{\mathrm{Ru_2^{II,III}}\}^+]$.

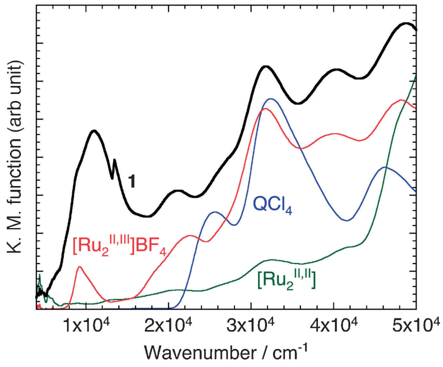

Figure 3. Powder reflection spectra of **1** (black), $\mathrm{QCl_4}$ (blue), $[\mathrm{Ru_2^{II,II}}(o\text{-}\mathrm{MeOPhCO_2})_4(\mathrm{THF})_2]$ (green), and $[\mathrm{Ru_2^{II,III}}(o\text{-}\mathrm{MeOPhCO_2})_4(\mathrm{THF})_2]\mathrm{BF_4}$ (red) measured based on a $\mathrm{BaSO_4}$ pellet.

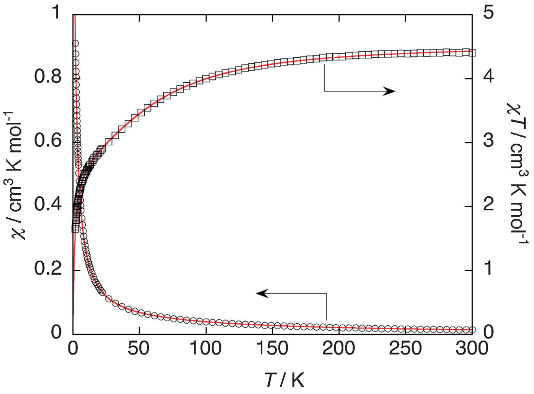

Figure 4. Temperature dependence of χ and χT of **1**, where the red solid lines represent best-fit curves using a Curie paramagnetic model for $S = 3/2$ with parameters noted in the text.

This conclusion on the charge distribution is supported by the magnetic behavior. χ and χT vs. T plots for **1** are shown in Figure 4. The χT value of $4.40\,\mathrm{cm^3\,K\,mol^{-1}}$ at 300 K continuously decreased to $1.65\,\mathrm{cm^3\,K\,mol^{-1}}$ at 1.8 K. The characteristic value at 300 K and a monotonic decrease of χT with relatively large values at low temperatures indicate that this behavior displays the paramagnetic nature of $[\mathrm{Ru_2^{II,III}}]^+$ mediated by a diamagnetic $\mathrm{QCl_4^{2-}}$.[30] The χ and χT values were simulated in the entire temperature range by using a Curie paramagnetic model with $S = 3/2$ involving zero-field splitting (D), temperature-independent paramagnetism (χ_{TIP}), and intermolecular interactions (zJ) commonly used for magnetically isolated or weakly interacting $[\mathrm{Ru_2^{II,III}}]^+$ complexes.[1,2,7,8g] zJ was introduced in the framework of the mean-field approximation (z = number of adjacent magnetic centers, assuming $z = 1$ for this case). The best fit of parameters were: $g = 2.191(2)$, $D/k_{\mathrm{B}} = 101.9(7)\,\mathrm{K}$, $J/k_{\mathrm{B}} = -0.795(5)\,\mathrm{K}$, and $\chi_{\mathrm{TIP}} = 52(16) \times 10^{-6}\,\mathrm{cm^3\,mol^{-1}}$ with $R = 1 - \Sigma[(\chi T_{\mathrm{calc}} - \chi T_{\mathrm{obs}})^2 \Sigma(\chi T_{\mathrm{obs}})]^2 = 0.99998$ (fitted curves are red in Figure 4). The obtained values of g, which are larger than 2.00, and D are typical for $[\mathrm{Ru_2^{II,III}}]^+$ complexes[1,2,7,8g] and in good agreement with the values ($g = 2.2607(8)$, $D/k_{\mathrm{B}} = 106.4(6)\,\mathrm{K}$, $J/k_{\mathrm{B}} \approx 0\,\mathrm{K}$, and $\chi_{\mathrm{TIP}} = 34(11) \times 10^{-6}\,\mathrm{cm^3\,mol^{-1}}$) for $[\mathrm{Ru_2^{II,III}}(o\text{-}\mathrm{MeOPhCO_2})_4(\mathrm{THF})_2]$-

BF_4 (Figure S4[33]). The small J value indicates that the $[Ru_2^{II,III}]^+$ units are almost magnetically isolated, although the present exchange should be attributed to a superexchange via QCl_4^{2-}. This magnetic nature with a weak superexchange via QCl_4^{2-} was also found in $[Fe(tpp)]_2(QCl_4)$.[29]

In conclusion, the reaction between $[Ru_2^{II,II}(o\text{-}MeOPhCO_2)_4(THF)_2]$ and QCl_4 occurs a full charge transfer to form divalent tetrachlorohydroquinonate (QCl_4^{2-}), which is stabilized in a formation of neutral dimer-of-dimers with an array of [THF–$\{Ru_2^{II,III}\}$–(QCl_4^{2-})–$\{Ru_2^{II,III}\}$–THF]. This charge distribution is very likely because the $[Ru_2^{II,II}(o\text{-}MeOPhCO_2)_4(THF)_2]$ unit has a significantly small ionization potential, which can overcome an on-site Coulomb repulsion on QCl_4. Indeed, the HOMO level of $[Ru_2^{II,II}(o\text{-}MeOPhCO_2)_4\text{-}(THF)_2]$ calculated based on atomic coordinates from X-ray crystallography using basic functions of UB3LYP/LANL2TZ(f) for Ru and 6-31+G* for other elements is −3.727 eV (δ^* character with β spin), which is much higher than −4.133 eV and −4.162 for $[Ru_2^{II,II}(PhCO_2)_4(THF)_2]$[16] and $[Ru_2^{II,II}(o\text{-}MePhCO_2)_4(THF)_2]$,[8g] respectively. Thus, the formation of two-electron-transferred species QCl_4^{2-} is quite reasonable, because the LUMO level of QCl_4^0 (−4.642 eV)[31] is significantly lower than the HOMO level of $[Ru_2^{II,II}(o\text{-}MeOPhCO_2)_4(THF)_2]$ as was seen in a set of $[Ru_2(m\text{-}MePhCO_2)_4(THF)_2]$ and BTDA-TCNQ ($m\text{-}MePhCO_2^-$: *m*-methylbenzoate; BTDA-TCNQ: bis(1,2,5-thiadiazolo)tetracyanoquinodimethane) that led to a two-electron transfer in a D_2A system.[8g] Finally, it is noteworthy that the present material is the first of charge-transferred assembly derived by the reaction of paddlewheel $[Ru_2^{II,II}]$ units with benzoquinone derivatives.[32]

This work was financially supported by a Grant-in-Aid for Scientific Research from the Ministry of Education, Culture, Sports, Science and Technology, Japan (Grant No. 21350032).

References and Notes

1 M. A. S. Aquino, *Coord. Chem. Rev.* **1998**, *170*, 141.

2 M. Mikuriya, D. Yoshioka, M. Handa, *Coord. Chem. Rev.* **2006**, *250*, 2194.

3 a) Y. Liao, W. W. Shum, J. S. Miller, *J. Am. Chem. Soc.* **2002**, *124*, 9336. b) T. E. Vos, Y. Liao, W. W. Shum, J.-H. Her, P. W. Stephens, W. M. Reiff, J. S. Miller, *J. Am. Chem. Soc.* **2004**, *126*, 11630.

4 a) D. Yoshioka, M. Mikuriya, M. Handa, *Chem. Lett.* **2002**, 1044. b) T. E. Vos, J. S. Miller, *Angew. Chem., Int. Ed.* **2005**, *44*, 2416.

5 J. S. Miller, T. E. Vos, W. W. Shum, *Adv. Mater.* **2005**, *17*, 2251.

6 H. Miyasaka, Y. Asai, N. Motokawa, K. Kubo, M. Yamashita, *Inorg. Chem.* **2010**, *49*, 9116.

7 H. Miyasaka, R. Clérac, C. S. Campos-Fernández, K. R. Dunbar, *Inorg. Chem.* **2001**, *40*, 1663.

8 a) H. Miyasaka, C. S. Campos-Fernández, R. Clérac, K. R. Dunbar, *Angew. Chem., Int. Ed.* **2000**, *39*, 3831. b) H. Miyasaka, T. Izawa, N. Takahashi, M. Yamashita, K. R. Dunbar, *J. Am. Chem. Soc.* **2006**, *128*, 11358. c) N. Motokawa, T. Oyama, S. Matsunaga, H. Miyasaka, K. Sugimoto, M. Yamashita, N. Lopez, K. R. Dunbar, *Dalton Trans.* **2008**, 4099. d) N. Motokawa, H. Miyasaka, M. Yamashita, K. R. Dunbar, *Angew. Chem., Int. Ed.* **2008**, *47*, 7760. e) N. Motokawa, T. Oyama, S. Matsunaga, H. Miyasaka, M. Yamashita, K. R. Dunbar, *CrystEngComm* **2009**, *11*, 2121. f) H. Miyasaka, N. Motokawa, S. Matsunaga, M. Yamashita, K. Sugimoto, T. Mori, N. Toyota, K. R. Dunbar, *J. Am. Chem. Soc.* **2010**, *132*, 1532. g) H. Miyasaka, T. Morita, M. Yamashita, *Chem. Commun.* **2011**, *47*, 271.

9 N. Motokawa, H. Miyasaka, M. Yamashita, *Dalton Trans.* **2010**, *39*, 4724.

10 H. Miyasaka, N. Motokawa, T. Chiyo, M. Takemura, M. Yamashita, H. Sagayama, T.-h. Arima, *J. Am. Chem. Soc.* **2011**, *133*, 5338.

11 Elemental analysis (%) calcd for $C_{40}H_{44}O_{14}Ru_2$: C, 50.52; H, 4.66%. Found: C, 50.44; H, 4.60%. The crystal structure was determined by single-crystal X-ray crystallography as given in Figure S1[33] and CCDC-846070.

12 Compound **1** was synthesized as microcrystals refluxing under anaerobic conditions in a benzene solution (200 mL) of QCl_4 (78.4 mg, 0.32 mmol) for 89 h in a bottom-rounded Schlenk flask attached to a Soxhlet extractor containing a solid of $[Ru_2^{II,II}(o\text{-}MeOPhCO_2)_4(THF)_2]$ (608.4 mg, 0.64 mmol). During refluxing, brown microcrystals were precipitated. Yield: 32.8 mg, 10.2%. Elemental analysis (%). Calcd for **1**, $C_{78}H_{72}Cl_4O_{28}Ru_4$: C, 46.8; H, 3.62%. Found: C, 47.1; H, 3.61%. The crystal samples suitable for X-ray crystallography were prepared using a slow diffusion technique.

13 Crystallographic data of **1**. $C_{78}H_{72}Cl_4O_{28}Ru_4$, $M_r = 2003.50$, Monoclinic, $P2_1/n$ (#14), $a = 14.207(3)$ Å, $b = 17.841(3)$ Å, $c = 15.491(3)$ Å, $\beta = 94.589(2)°$, $V = 3913.7(11)$ Å^3, $T = 103$ K, $Z = 2$, $D_{calcd} = 1.700$ g cm^{-3}, $F_{000} = 2016.00$, $\lambda = 0.71070$ Å, $\mu(\text{Mo K}\alpha) = 9.772$ cm^{-1}, 25534 measured reflections, 6799 unique ($R_{int} = 0.0228$). $R_1 = 0.0423$ ($I > 2\sigma(I)$), $R_1 = 0.0492$ (all data), and $wR_2 = 0.1142$ (all data) with GOF = 1.096. CCDC-846069.

14 a) M. Handa, D. Yoshioka, Y. Sayama, K. Shiomi, M. Mikuriya, I. Hiromitsu, K. Kasuga, *Chem. Lett.* **1999**, 1033. b) D. Yoshioka, M. Mikuriya, M. Handa, *Bull. Chem. Soc. Jpn.* **2004**, *77*, 2205. c) D. Yoshioka, M. Handa, H. Azuma, M. Mikuriya, I. Hiromitsu, K. Kasuga, *Mol. Cryst. Liq. Cryst.* **2000**, *342*, 133.

15 *Multiple Bonds between Metal Atoms*, 2nd ed., ed. by F. A. Cotton, R. A. Walton, Oxford University Press, Oxford, **1993**.

16 H. Miyasaka, N. Motokawa, R. Atsuumi, H. Kamo, Y. Asai, M. Yamashita, *Dalton Trans.* **2011**, *40*, 673.

17 S. S. C. Chu, G. A. Jeffrey, T. Sakurai, *Acta Crystallogr.* **1962**, *15*, 661.

18 S. H. Kim, W. T. Lim, N. H. Heo, *Dyes Pigm.* **1999**, *41*, 89.

19 K. Kozawa, T. Uchida, *Acta Crystallogr., Sect. C: Cryst. Struct. Commun.* **1983**, *39*, 1233.

20 K. Yakushi, I. Ikemoto, H. Kuroda, *Acta Crystallogr., Sect. B: Struct. Crystallogr. Cryst. Chem.* **1973**, *29*, 2640.

21 I. J. Tickle, C. K. Prout, *J. Chem. Soc., Perkin Trans. 2* **1973**, 724.

22 K. Nakasuji, M. Sasaki, T. Kotani, I. Murata, T. Enoki, K. Imaeda, H. Inokuchi, A. Kawamoto, J. Tanaka, *J. Am. Chem. Soc.* **1987**, *109*, 6970.

23 G. Zanotti, A. Del Pra, *Acta Crystallogr., Sect. B: Struct. Crystallogr. Cryst. Chem.* **1980**, *36*, 313.

24 E. J. Brandon, R. D. Rogers, B. M. Burkhart, J. S. Miller, *Chem.—Eur. J.* **1998**, *4*, 1938.

25 J. L. de Boer, A. Vos, *Acta Crystallogr., Sect. B: Struct. Crystallogr. Cryst. Chem.* **1968**, *24*, 720.

26 S. K. Sikka, R. Chidambaram, *Acta Crystallogr.* **1967**, *23*, 107.

27 A. L. Rheingold, private communication in CCDC-213348.

28 Elemental analysis (%). Calcd for $[Ru_2(o\text{-}MeOPhCO_2)_4(THF)_2]\text{-}BF_4\cdot 2H_2O$, $C_{40}H_{48}BF_4O_{16}Ru_2$: C, 44.74; H, 4.51%. Found: C, 45.04; H, 4.67%. The crystal structure was determined by single-crystal X-ray crystallography as given in Figure S3[33] and CCDC-846071.

29 S. L. Kessel, D. N. Hendrickson, *Inorg. Chem.* **1980**, *19*, 1883.

30 The χT values at low temperatures for isolated $[Ru_2^{II,II}]$ complexes are much smaller than those for $[Ru_2^{II,III}]^+$ owing to the effect of larger zero-field splitting ($D/k_B = 340\text{–}420$ K for $[Ru_2^{II,II}]$) than for $[Ru_2^{II,III}]^+$. See refs 15 and 16.

31 For the calculations for QCl_4^0, the atomic coordinates computer-optimized were used.

32 Handa, Mikuriya, et al. have reported a possible example of charge-transferred compounds, $[Ru_2(O_2CC(CH_3)_3)_4(9,10\text{-}aq)]_n$ (9,10-aq: 9,10-anthraquinone), in refs 14c and 2, but the details of it, even charge distribution between $[Ru_2]$ unit and 9,10-aq, were still unexplained.

33 Supporting Information is available electronically on the CSJ-Journal Web site, http://www.csj.jp/journals/chem-lett/index.html.